Sustainable Energy, Grids and Networks 32 (2022) 100895

Contents lists available at ScienceDirect

Sustainable Energy, Grids and Networks

journal homepage: www.elsevier.com/locate/segan

A fast non-decoupled algorithm to solve the load flow problem in meshed distribution networks

Hugo Edgardo Hernández-Fuentes *, Francisco Javier Zarco Soto, José Luis Martínez-Ramos

Department of Electrical Engineering, University of Seville, Sevilla, Spain

ARTICLE INFO

Article history:
Received 9 December 2021
Received in revised form 7 April 2022
Accepted 29 July 2022
Available online 10 August 2022

Keywords:
Power flow
Distribution system

ABSTRACT

The purpose of this work is to compare the classical methods of power flow resolution (Newton–Raphson and Gauss–Seidel) with a more recent algorithm known as Alternating Search Direction (ASD), for which its equations, the steps to follow and the parameters to consider are described. In addition, a series of tests are carried out in different distribution networks where the reduction of execution time, accuracy, and robustness of the presented algorithm is demonstrated, taking as a reference the behavior of the well-known Newton–Raphson algorithm. Finally, the advantage of selecting certain parameters in the ASD algorithm is studied.

1. Introduction

Since the beginning of electrical power systems, the Load Flow Problem has been necessary to determine their correct operation and planning. These studies determine the magnitudes of the voltage and phase angle in each system bus, given the loads and generations in the system. For this purpose, different resolution methods have been developed over the years, such as the classical Gauss–Seidel and Newton–Raphson methods [1–3], in which several alternatives have been proposed to reduce computational effort and execution times, as well as to avoid convergence problems due to the characteristics of the network [4] (i.e., meshed transmission networks and radially operated distribution networks), with the aim of being applicable to new challenges arising in electric grids such as the inclusion of the electric vehicle [5–7], isolated microgrids [8–10], and the inclusion of solar energy [11], to mention a few. This objective of improving the resolution of the power flow problem for the new elements included in the networks motivates this work to propose a robust resolution method, especially oriented to distribution networks.

1.1. Related work

Historically, power flow resolution started with the classical Gauss–Seidel method, followed by the Newton–Raphson method; the latter is the origin of the well-known Fast Decoupled Load Flow algorithm [12], and several load flow methods that take advantage of the characteristics of the transmission network [13]. In contrast, tree-sweep-based methods, such as the impedance matrix-based method, take advantage of the radial characteristics of distribution systems [14]. Numerous methods have been developed to calculate power flow in distribution networks [15,16], including unbalanced three-phase load flow methods, which, despite their high convergence rate, require linearization of equations due to their high R/X ratio [17–19]. Algorithms have also been developed to solve hybrid AC–DC distribution networks combining the advantages of both the Gauss–Seidel and Newton–Raphson methods [20,21]. However, depending on the type of network, these methods may present convergence problems or require a significant amount of computational effort, especially when dealing with voltage control devices [22–24] and how to update the Jacobian in each iteration [25–28]. In addition, several algorithms have been proposed to solve transmission and distribution systems simultaneously [29], due to the increasing distributed generation that influences the flow from distribution networks to the transmission network [30,31].

1.2. Contributions and organization

The objective of this paper is to propose an alternative method to solve the load flow problem in distribution networks, comparing its behavior with the classical Gauss–Seidel and Newton–Raphson methods, to demonstrate that this method can be an attractive alternative that saves computational time and effort due to its simplicity, compared to current methods that are based on assumed simplifications that are not always valid in a context of increasing distributed generation and the operation of distribution networks in a meshed configuration. Furthermore, this method can be used in both meshed and radial networks,

* Corresponding author.
E-mail address: hugherfue@alum.us.es (H.E. Hernández-Fuentes).

https://doi.org/10.1016/j.segan.2022.100895

Nomenclature

$[l+\frac{1}{2}]$	Superscript indicating the Global step at iteration l.
$[l]$	Superscript indicating the Local step at iteration l.
$\boldsymbol{\alpha}$	Global step direction search vector.
$\boldsymbol{\beta}$	Local step direction search vector.
ΔI_c	PQ nodes current corrections.
ΔI_g	PV nodes current corrections.
ΔI_s	Slack bus current corrections.
ΔV_c	PQ nodes voltage corrections.
ΔV_g	PV nodes voltage corrections.
ΔV_s	Slack node voltage correction.
$\mathbf{Y_r}$	Reduced $\mathbf{Y_{bus}}$ matrix.
I	Vector of currents.
I_0	Vector of slack current contributions.
Q_g	Reactive powers of PV nodes.
S	Vector of complex powers.
V	Vector of voltages.
Y_{cc}	Admittance matrix of PQ nodes.
Y_{gc}	Admittance matrix between PV and PQ nodes.
Y_{gg}	Admittance matrix of the PV nodes.
Y_{sc}	Admittance vector between the slack and PQ nodes.
Y_{sg}	Admittance vector between the slack and PV nodes.
Y_{ss}	Slack bus admittance.

in contrast to other methods that are only suitable for radial networks [32,33], thus contributing to the development of a new set of methods for the resolution of load flows in distribution networks [34].

The paper is structured as follows. Section 2 presents the mathematical equations of the Alternating Search Directions (ASD) algorithm, together with the parameters that control the convergence of the algorithm. Section 3 presents a comparative example in which control parameters are modified to improve convergence and execution times. Then, the ASD algorithm is used to solve different distribution networks to check the behavior and robustness of this algorithm compared to classical methods. The paper ends with the presentation of the conclusions in Section 4.

2. Method of alternating search directions

The algorithm proposed to solve the load flow problem is the Alternating Search Direction method [35,36]. In [37] the ASD method is applied to non-linear structural mechanical problems, where the theory of the method is detailed. The method starts from Kirchhoff's current equations for all buses except the Slack Bus, and the corresponding complex power balances, as shown below.

$$\mathbf{Y_r}\, V = I + I_0 \tag{1}$$

$$S = V \odot I^* \tag{2}$$

where I_0 is a vector of current contributions from the Slack Bus to the adjacent buses, since the Slack Bus is transformed into current sources connected to the adjacent buses [38], and $\mathbf{Y_r}$ is the reduced matrix $\mathbf{Y_{bus}}$ that does not include the slack bus. By combining Eqs. (1) and (2), the following equations are obtained.

$$\mathbf{Y_r}\, V = (S \oslash V)^* + I_0 \tag{3}$$

$$S^* = V^* \odot (\mathbf{Y_r}\, V - I_0) \tag{4}$$

The ASD method proposes that, when obtaining Eq. (3), the global linear problem (1) is combined with nonlinear local constraints (2) [39]. In this way, the algorithm solves in each iteration the nonlinear system of equations in two steps, using linear relationships between voltages and currents, that is, the direction of the search matrices ($\boldsymbol{\alpha}$ and $\boldsymbol{\beta}$). Therefore, the first step of iteration l consists of solving the following system of equations,

$$\begin{cases} I^{[l+\frac{1}{2}]} - I^{[l]} = \boldsymbol{\alpha}\left(V^{[l+\frac{1}{2}]} - V^{[l]}\right) \\ \mathbf{Y_r}\, V^{[l+\frac{1}{2}]} = I_0 + I^{[l+\frac{1}{2}]} \end{cases} \tag{5}$$

Similarly, the second step consists of the following system of equations.

$$\begin{cases} I^{[l+1]} - I^{[l+\frac{1}{2}]} = \boldsymbol{\beta}\left(V^{[l+1]} - V^{[l+\frac{1}{2}]}\right) \\ V^{[l+1]*} \odot I^{[l+1]} = S^* \end{cases} \tag{6}$$

As a consequence, the algorithm is based on solving a "Global Step" first in each iteration, defined by Eq. (7),

$$(\mathbf{Y_r} - \boldsymbol{\alpha})\; V^{[l+\frac{1}{2}]} = \left(S \oslash V^{[l]}\right)^* - \boldsymbol{\alpha}\, V^{[l]} + I_0 \tag{7}$$

followed by a "Local Step", defined by Eq. (8),

$$\boldsymbol{\beta}\, V^{[l+1]} + \left[(\mathbf{Y_r} - \boldsymbol{\beta})\; V^{[l+\frac{1}{2}]} - I_0\right] - \left(S \oslash V^{[l+1]}\right)^* = 0 \tag{8}$$

2.1. Selection of matrices $\boldsymbol{\alpha}$ and $\boldsymbol{\beta}$

The search direction for the Global Step, $\boldsymbol{\alpha}$, is selected as follows:

$$\boldsymbol{\alpha} = \mathrm{diag}\left(S^* \oslash |V_b|^2\right) \tag{9}$$

where V_b represents the base voltage, approximated in *per unit* by $V_b = 1$. This approximation allows us to modify the admittance matrix in the Global Step to include the linear model of the loads ($\mathbf{Y_r} - \boldsymbol{\alpha}$). Regarding the search direction in the local step, most methods select $\boldsymbol{\beta} \to \infty$, which implies that the voltage of the Local Step is inherited from the Global Step. Therefore, a more appropriate option to select $\boldsymbol{\beta}$ would be the following:

$$\boldsymbol{\beta} = \mathrm{diag}\,(\mathbf{Y_r} - \boldsymbol{\alpha}) \tag{10}$$

This allows $\boldsymbol{\beta}$ to have a better spectral approximation of $\mathbf{Y_r}$. In addition, a good selection for $\boldsymbol{\beta}$ can also be made as

$$\boldsymbol{\beta} = \mathrm{diag}\left([\mathbf{Y_r} - \boldsymbol{\alpha}]^{-1}\right)^{-1} \tag{11}$$

To avoid convergence problems caused by the matrix resulting from $(\mathbf{Y_r} - \boldsymbol{\alpha})$ being singular, $\boldsymbol{\alpha} = -\boldsymbol{\beta}^{-1}$ may also be selected. However, this selection does not imply any advantage when performing the calculations in the algorithm.

2.2. Treatment of PV nodes

Unlike other load flow algorithms, which treat the PV nodes at the end of each iteration, in the ASD algorithm, this is done at the end of the Global Step. With the voltage vector obtained in the Global Step, it is clear that $|V^{[l+\frac{1}{2}]}| \neq E_{\mathrm{spe}}$, where E_{spe} is the

expected voltage magnitude at the PV node. Using the admittance matrix, we can relate the current changes to the voltage changes,

$$\begin{bmatrix} \Delta I_s \\ \Delta I_g \\ \Delta I_c \end{bmatrix} = \begin{bmatrix} Y_{ss} & Y_{sg} & Y_{sc} \\ Y_{gs} & Y_{gg} & Y_{gc} \\ Y_{cs} & Y_{cg} & Y_{cc} \end{bmatrix} \begin{bmatrix} \Delta V_s \\ \Delta V_g \\ \Delta V_c \end{bmatrix}$$

Since for the Slack Bus $\Delta V_s = 0$, and initially $\Delta I_c = 0$ for the load nodes, we can obtain ΔV_c, which corresponds to the loads, and ΔI_g for the PV buses due to voltage corrections in the PV nodes. As a consequence, we obtain the following equations:

$$\Delta V_g = V_{\text{spe}} - V_g \tag{12}$$

$$\Delta V_c = -\mathbf{Y_{cc}^{-1}}\,\mathbf{Y_{cg}}\,\Delta V_g \tag{13}$$

$$\Delta I_g = \left[\mathbf{Y_{gg}} - \mathbf{Y_{gc}}\,\mathbf{Y_{cc}^{-1}}\,\mathbf{Y_{cg}}\right]\,\Delta V_g \tag{14}$$

Starting by applying a Kron reduction [1] to $\mathbf{Y_r}$ to calculate ΔI_g in (14), we can obtain the required corrections in the current of PV buses to keep the voltages as expected,

$$\Delta I_g = \mathbf{Y}_{\text{Kron}}\,\Delta V_g \tag{15}$$

To calculate ΔV_g first, V_{spe} is obtained, which is the scheduled value of the voltage magnitude, keeping the phase calculated in the global step. Once Eqs. (12)–(14) are solved, I_g, V_c, and V_g are known, the latter being the voltages that form the vector $V^{[l+\frac{1}{2}]}$ of the updated Global Step. Once I_g and V_g are obtained, the reactive power of PV buses is calculated according to (16).

$$Q_g = \Im\left(V_g \odot I_g^*\right) \tag{16}$$

2.3. ASD algorithm

The ASD algorithm is detailed below (see also Fig. 1).

(1) Obtain the admittance matrix $\mathbf{Y_r}$, in addition to the vectors S and I_0 of the system.
(2) Select the search directions matrices $\boldsymbol{\alpha}$ and $\boldsymbol{\beta}$.
(3) Evaluate the starting point for voltages V^0.
(4) Start the iterative process between the Global Step and the Local Step.
(5) In each iteration, evaluate $|V^{[l+\frac{1}{2}]} - V^{[l+1]}|$ until it is less than a convergence tolerance ϵ.

2.4. Advantages of the ASD algorithm

- The Global Step is linear, while the local step is nonlinear and generates two valid solutions. The voltage solution that provides the highest value when solving the Local Step must be selected.
- The search directions $\boldsymbol{\alpha}$ and $\boldsymbol{\beta}$ must be calculated only once, and the corresponding matrices are inverted only in the initialization process.
- Both the Global Step solution and the Local Step solution meet the equations of (1) and (2), so $(V, I)^{[l+\frac{1}{2}]} \equiv (V, I)^{[l+1]}$ which implies that they comply with Eq. (3), which allows them to be used to control convergence, $|V^{[l+\frac{1}{2}]} - V^{[l+1]}|$.

2.5. Particularizations of the method

By defining the $\boldsymbol{\alpha}$ and $\boldsymbol{\beta}$ search directions, it can be shown that the Gauss–Seidel and Newton–Raphson methods are particularizations of the Alternating Search Direction method, with these demonstrations as follows.

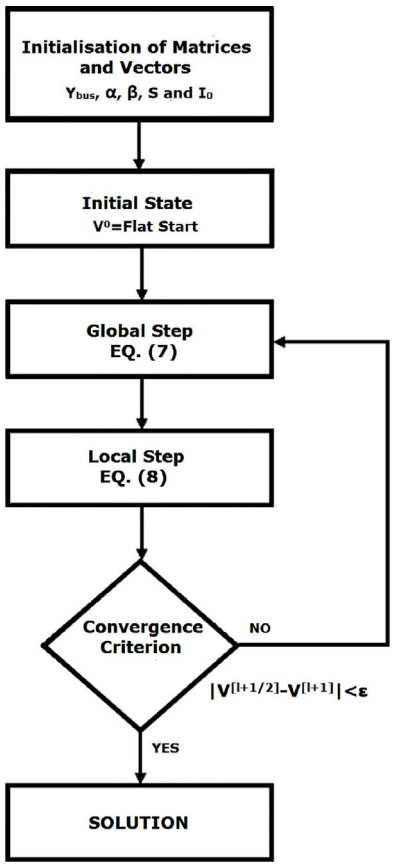

Fig. 1. Alternating search direction algorithm.

2.5.1. Gauss–Seidel algorithm

Selecting $\boldsymbol{\beta} \to \infty$ and $\boldsymbol{\alpha} = \mathbf{Y_{rU}}$, which is the upper triangular part of the reduced matrix $\mathbf{Y_{bus}}$ without diagonal elements, and, on the other hand, $\mathbf{Y_{rL}} = \mathbf{Y_r}$ - $\boldsymbol{\alpha}$ is the lower triangular one, we can also consider $V^{[l+1]} \to V^{[l+\frac{1}{2}]}$, which allows us to reduce the equation scheme of the Alternating Search Directions method to Eq. (17).

$$\begin{aligned} V^{[l+1]} &= V^{[l+\frac{1}{2}]} \\ &= \mathbf{Y_{rL}}^{-1}\left[\left(S \oslash V^{[l]}\right)^* - \mathbf{Y_{rU}}\,V^{[l]} + I_0\right] \end{aligned} \tag{17}$$

Eq. (17) is the classical formulation of the Gauss–Seidel algorithm.

2.5.2. Newton–Raphson algorithm

In order to formally define the Newton–Raphson method as a particularization of the Alternating Search Direction method, it is necessary that the equation of current injections at the nodes (3) is formulated with the voltages in its rectangular form by separating the real and imaginary parts and using $\mathbf{Y_r} = \mathbf{G_r} + \mathrm{j}\mathbf{B_r}$, which allows us to define

$$\mathbf{M} = \begin{bmatrix} \mathbf{G_r} & -\mathbf{B_r} \\ \mathbf{B_r} & \mathbf{G_r} \end{bmatrix} \tag{18}$$

$$W = \begin{bmatrix} V_{Re} \\ V_{Im} \end{bmatrix} \tag{19}$$

$$\begin{aligned} N &= \begin{bmatrix} N_{Re} \\ N_{Im} \end{bmatrix} = \\ &= \begin{bmatrix} I_{0Re} + (P \odot V_{Re} + Q \odot V_{Im}) \oslash (V_{Re}^2 + V_{Im}^2) \\ I_{0Im} + (P \odot V_{Im} - Q \odot V_{Re}) \oslash (V_{Re}^2 + V_{Im}^2) \end{bmatrix} \end{aligned} \tag{20}$$

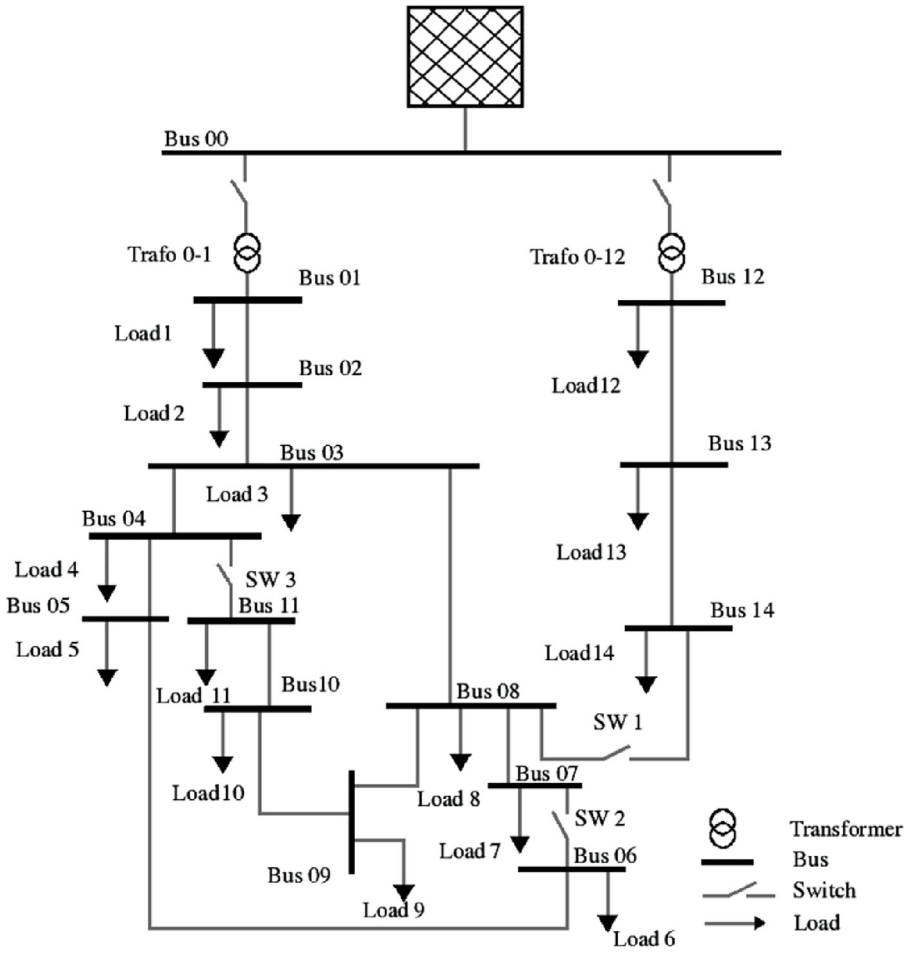

Fig. 2. CIGRE MV network.

which allows us to write the power equations as follows.

$$\mathbf{M}\,W = N \tag{21}$$

Then select the search directions $\boldsymbol{\beta} \to \infty$, and $\boldsymbol{\alpha}$ as follows:

$$\boldsymbol{\alpha} = \begin{bmatrix} \frac{\partial N_{Re}}{\partial V_{Re}} & \frac{\partial N_{Re}}{\partial V_{Im}} \\ \frac{\partial N_{Im}}{\partial V_{Re}} & \frac{\partial N_{Im}}{\partial V_{Im}} \end{bmatrix} \tag{22}$$

The last consideration is to select $W^{[l+1]} \to W^{[l+\frac{1}{2}]}$, which allows us to conclude with the Newton–Raphson algorithm defined in Eq. (23).

$$W^{[l+1]} = W^{[l+\frac{1}{2}]} = W^{[l]} - (\mathbf{M} - \boldsymbol{\alpha})^{-1}(\mathbf{M}\,N^{[l]} - N^{[l]}) \tag{23}$$

3. Comparison of algorithms

In this paper, the comparison between the ASD algorithm and Newton–Raphson and Gauss–Seidel algorithms is focused on the execution time and the robustness of convergence in different networks. For the ASD algorithm, two different approaches for $\boldsymbol{\beta}$ are compared, $\boldsymbol{\beta} \to \infty$ and $\boldsymbol{\beta}$ selected according to (11). The networks used as test cases are the CIGRE distribution network [40,41], a 33-bus test system [42], a 69-bus system [43], a 141-bus system [44] and the IEEE European Low Voltage Test Feeder [45]. The tests were carried out in Matlab using a laptop with an Intel Core i5 8300H 2.30 GHz processor, 8 GB RAM, and Windows 10 Pro.

The performance of the algorithm is obtained by measuring the execution time of the algorithm and dividing it by the number of iterations until convergence. The reported execution time is an average of the execution times of the algorithm in 1000 executions for each network.

In the end, a robustness test of the ASD method is performed using the 415-bus distribution network [46], and a network with 10 476 buses artificially created using data from [47,48]. The differences in the solutions and the number of iterations compared with the results given by Newton–Raphson (NR) and Gauss–Seidel (GS) are presented.

3.1. Selection of $\boldsymbol{\beta} \to \infty$

The first example is the MV network proposed by CIGRE [20], which is a simple representation of a rural MV distribution network in Germany, which contains 15 nodes, two feeders, and 14 loads (Fig. 2).

Fig. 3 presents the total average execution time for the CIGRE network with a minimum demand state, where the NR performance is taken as a reference. GS presents a reduction in execution time of 76.53% while ASD has a reduction of 84.63%. For the same network but with maximum demand, a reduction of 75.89% for GS with respect to NR and 84.36% for ASD can be seen in Fig. 4. The total number of iterations and the total average execution times are also presented in Table 1, together with the results for other networks.

3.2. Selection of $\boldsymbol{\beta} \neq \infty$

The results obtained if $\boldsymbol{\beta}$ is selected as in Eq. (11) are presented in Figs. 5 and 6 for the CIGRE network, with minimum and

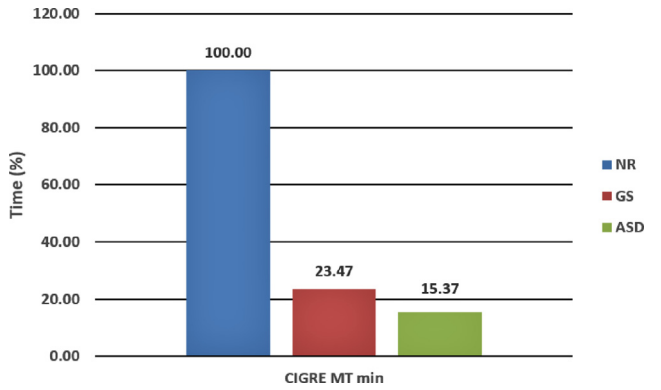

Fig. 3. Total execution times for the CIGRE network in a minimum load state.

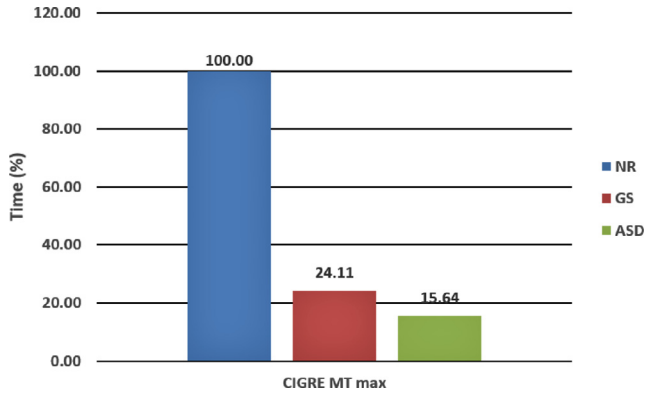

Fig. 4. Total execution times for the CIGRE network in a maximum load state.

Table 1
Test results with $\beta \to \infty$.

Network	Algorithm	Iterations	Percentage of time	Total time
CIGRE MT min	NR	3	100	0.029129
	GS	229	23.47	0.006835
	ASD	3	15.37	0.004477
CIGRE MT max	NR	3	100	0.028340
	GS	231	24.11	0.006833
	ASD	2	15.64	0.004434
33-Bus Network	NR	3	100	0.151209
	GS	126	8.71	0.013166
	ASD	4	7.17	0.010842
69-Bus Network	NR	5	100	1.247267
	GS	249	2.93	0.036485
	ASD	5	2.44	0.030394
141-Bus Network	NR	5	100	5.244316
	GS	3	1.42	0.074608
	ASD	4	1.53	0.080166
IEEE EU LV Network	NR	3	100	0.007818
	GS	No convergence		
	ASD	7	21 603.63	1.688946

maximum load, respectively. It can be seen that a reduction of about 84% is maintained when using the proposed ASD algorithm. The total number of iterations and the total average execution time are also presented in Table 2.

3.3. Tests results

Tables 1 and 2 present a summary of the results obtained in all tests for both cases, $\beta \to \infty$ and $\beta \neq \infty$, with a convergence tolerance of 10^{-4}. The percentage presented is measured with

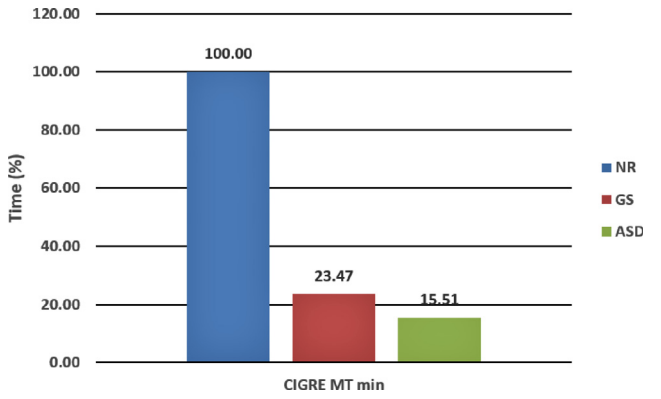

Fig. 5. Total execution times for the CIGRE network in a minimum load state and β selected as in Eq. (11).

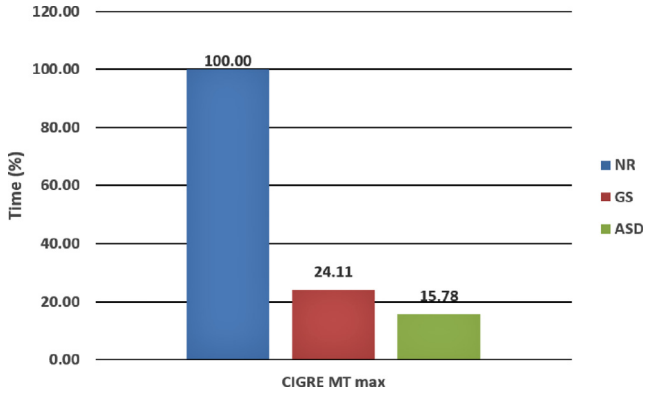

Fig. 6. Total execution times for the CIGRE network in peak load state and β selected as in Eq. (11).

respect to the execution time of the NR algorithm in order to show the time reduction that occurs in most cases, which is between 76% and 98% for GS, while for ASD is between 84% and 98%. In addition to verifying in most cases a significant reduction, it is also observed that the ASD algorithm tends to be faster than GS because it performs fewer iterations, with the exception of the 141-bus network in which it even beats NR in iterations; this is because, for the required accuracy, GS needs fewer iterations, but as the accuracy increases, the iterations that GS requires are greater, which translates into more time to find a solution. An example is observed in Figs. 7 and 8, where the execution time behavior with respect to different tolerances for the CIGRE network. In these figures, it is observed that GS is faster in networks that are heavily loaded and use low tolerances, while when a network is not heavily loaded or the required tolerance is high, the ASD algorithm tends to be better.

The last case analyzed in Tables 1 and 2 is the IEEE EU network, composed of 906 buses, which is assumed to be balanced, so one-phase data have been used for generalization. This network is the exception with respect to the execution time between NR and ASD, which shows that there is no perfect algorithm for all networks. Figs. 9 and 10 show the evolution of the voltage and angle of bus 619 through the iterative process, indicating the iteration on each label. Bus 619 is the one with the greatest difference between the response obtained by NR and the one given by ASD. The average time of each iteration was measured in both algorithms, 0.002 s for NR and 0.003 s for ASD, which is not significantly high for a network of 906 buses. It should be noted that the initialization time of the ASD matrices and vectors was analyzed, resulting in an average of 1.67 s, which shows that an

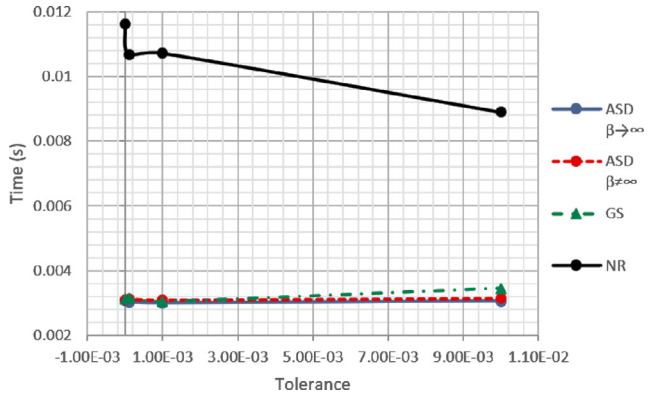

Fig. 7. Execution time versus tolerance for the CIGRE network in a peak load state.

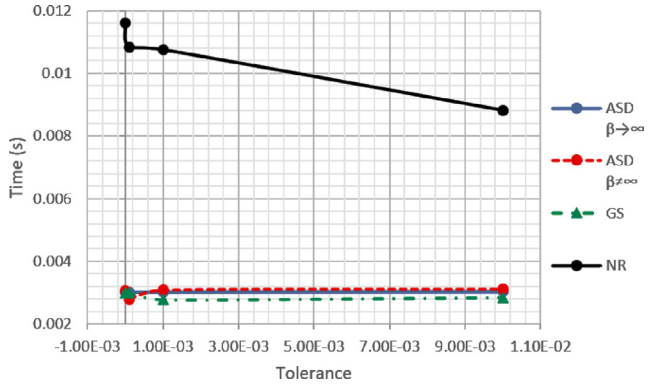

Fig. 8. Execution time versus tolerance for the CIGRE network in a minimum load state.

Table 2
Tests results with $\beta \neq \infty$.

Network	Algorithm	Iterations	Percentage of time	Total time
CIGRE MT min	NR	3	100	0.029129
	GS	229	23.47	0.006835
	ASD	3	15.51	0.004517
CIGRE MT max	NR	3	100	0.028340
	GS	231	24.11	0.006833
	ASD	2	15.78	0.004473
33-Bus Network	NR	3	100	0151209
	GS	126	8.71	0.013166
	ASD	4	7.30	0.011038
69-Bus Network	NR	5	100	1.247267
	GS	249	2.93	0.036485
	ASD	4	2.42	0.030125
141-Bus Network	NR	5	100	5.244316
	GS	3	1.42	0.074608
	ASD	4	1.50	0.078763
IEEE EU LV Network	NR	3	100	0.007818
	GS	No convergence		
	ASD	7	22 298.49	1.743269

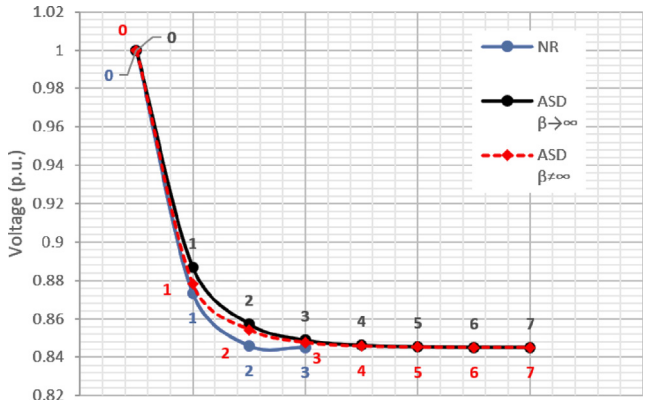

Fig. 9. Evolution of the voltage of bus 619 in each iteration of the EU network.

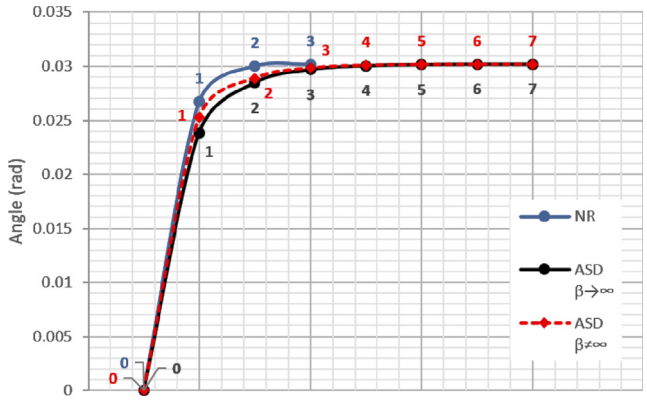

Fig. 10. Evolution of the angle of bus 619 in each iteration of the EU network.

Table 3
Results of the networks in radial configuration.

Network	Algorithm	Max difference V (p.u.)	Max difference Ang (rad)
415-Bus Network $\beta \to \infty$	GS	(Bus 8) 1.15888E−06	(Bus 8) 7.29452E−07
	ASD	(Bus 93) 1.78809E−06	(Bus 259) 1.30502E−06
415-Bus Network $\beta \neq \infty$	GS	(Bus 8) 1.15888E−06	(Bus 8) 7.29452E−07
	ASD	(Bus 93) 1.78809E−06	(Bus 259) 1.30502E−06
10 476-Bus Network $\beta \to \infty$	GS	No convergence	No convergence
	ASD	(Bus 5380) 8.90854E−06	(Bus 718) 1.14685E−05
10 476-Bus Network $\beta \neq \infty$	GS	No convergence	No convergence
	ASD	(Bus 5380) 8.90942E−06	(Bus 718) 1.14644E−05

improvement is needed in the construction of these matrices to achieve a more competitive execution time. Also, note that the GS algorithm fails to converge in this network.

3.4. Robustness of the method

The robustness test consists of taking the result obtained by NR as a reference and calculating the maximum difference between the GS and ASD solutions by identifying the bus where the greatest difference in both angle and voltage is achieved. The 415-bus network, composed of 55 feeders, 65 switches, and 480 branches, and the 10 476-bus network, composed of 84 feeders, 260 switches, and 10 736 branches, are used. Therefore, the test is performed in both radial and meshed configurations of the networks. The results are presented in Tables 3 and 4, where high precision is observed for both GS and ASD. Figs. 11 to 14 show the evolution through the iterative process of the voltages and angles of the nodes that present a greater difference between NR and ASD when the networks are configured radially. It should

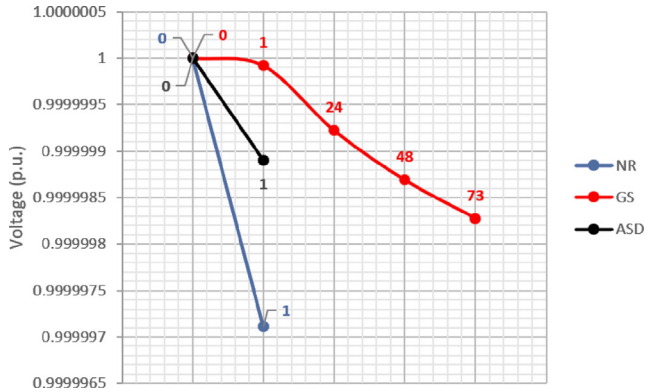

Fig. 11. Evolution of the voltage of bus 93 in the 415-bus network with radial configuration.

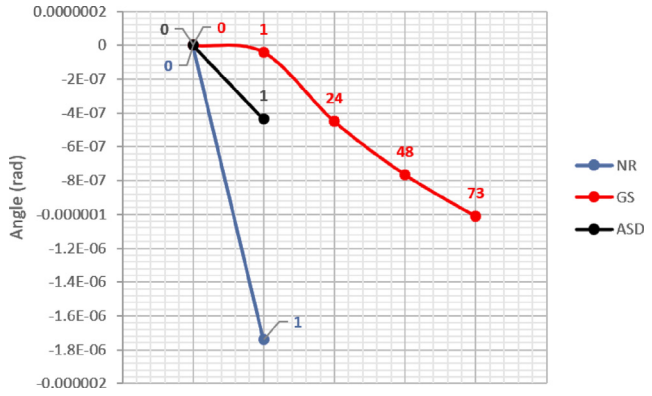

Fig. 12. Evolution of the angle of bus 259 in the 415-bus network with radial configuration.

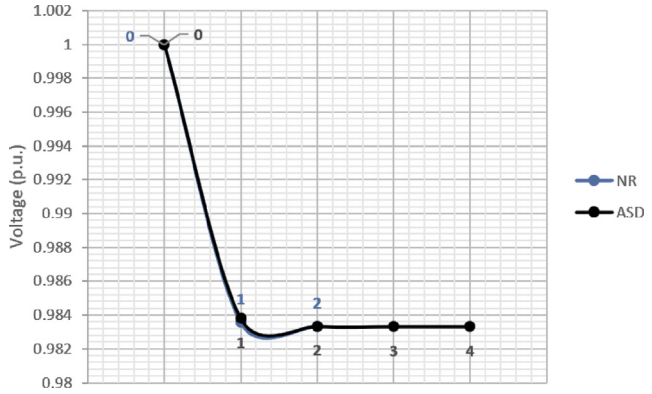

Fig. 13. Evolution of the voltage of bus 5380 in the 10 476-bus network with radial configuration.

be noted in Figs. 11 and 12, which correspond to the 415-bus network, even though the response achieved is not as accurate with GS with respect to NR, it is a robust response since the difference is given in amounts of 10^{-5} but with a smaller number of iterations, while for the 10 476-bus network it is observed that GS does not converge and ASD maintains a behavior similar to NR. If both networks are configured in a meshed way, Figs. 15 to 18, it is observed that there is an improvement in the accuracy achieved for the 415-bus network, Figs. 15 and 16, while for the 10 476-bus network, the same high accuracy is maintained, Figs. 17 and 18.

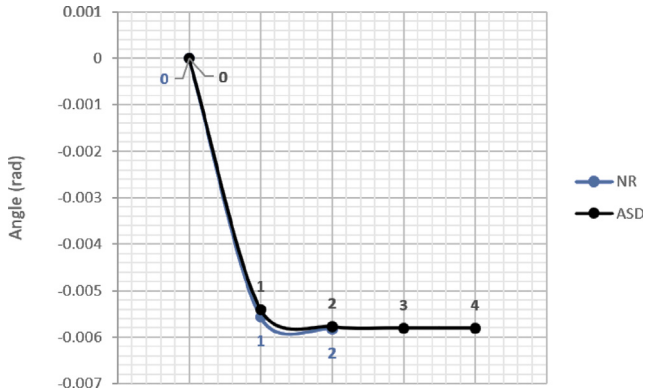

Fig. 14. Evolution of the angle of bus 718 in the 10 476-bus network with radial configuration.

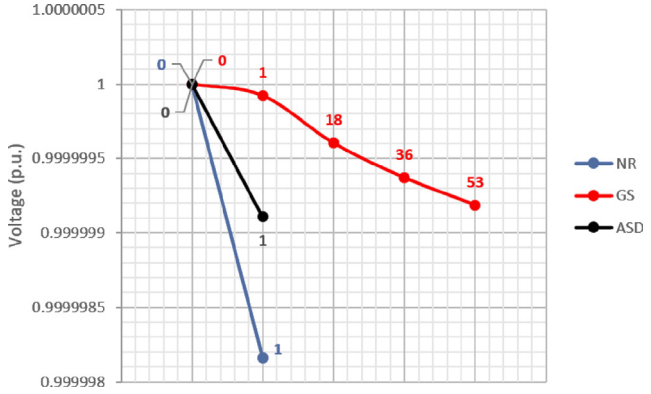

Fig. 15. Evolution of the voltage of bus 259 in the 415-bus network with a meshed configuration.

Table 4
Results of the networks in meshed configuration.

Network	Algorithm	Max difference V (p.u.)	Max difference Ang (rad)
415-Bus Network $\beta \to \infty$	GS	(Bus 63) 1.02869E−06	(Bus 63) 7.13506E−07
	ASD	(Bus 259) 9.45733E−07	(Bus 321) 1.92019E−07
415-Bus Network $\beta \neq \infty$	GS	(Bus 63) 1.02869E−06	(Bus 63) 7.13506E−07
	ASD	(Bus 259) 9.45733E−07	(Bus 321) 1.92019E−07
10 476-Bus Network $\beta \to \infty$	GS	No convergence	No convergence
	ASD	(Bus 8605) 7.21688E−06	(Bus 8658) 6.44443E−06
10 476-Bus Network $\beta \neq \infty$	GS	No convergence	No convergence
	ASD	(Bus 8605) 7.22591E−06	(Bus 8658) 6.44209E−06

4. Conclusions

The Alternating Search Directions (ASD) algorithm has proven to be a competitive load flow algorithm for distribution networks, based on comparisons with the classical Gauss–Seidel and Newton–Raphson methods. This has been demonstrated in the tests performed in the different networks presented in this paper, although there are critical cases, such as the European LV network, where the execution time is not reduced due to the

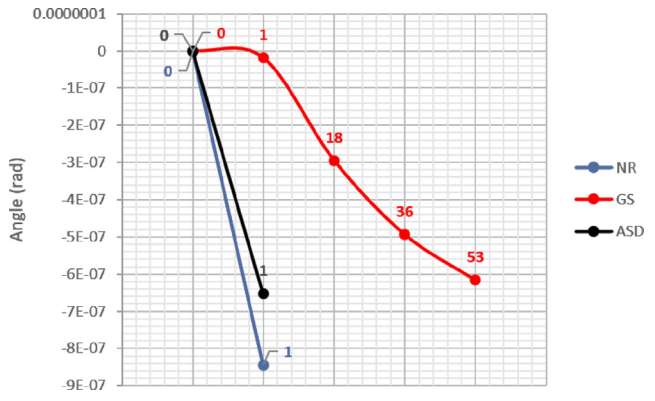

Fig. 16. Evolution of the angle of bus 321 in the 415-bus network with a meshed configuration.

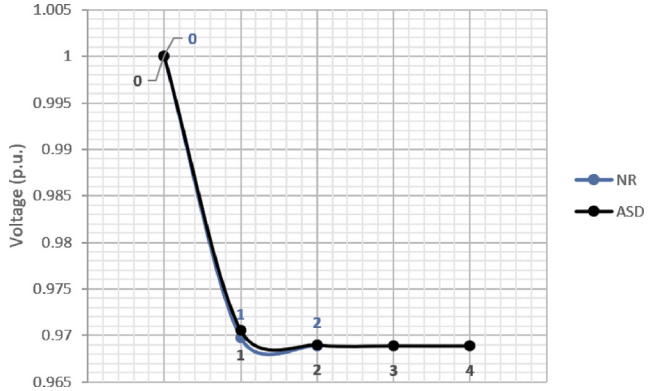

Fig. 17. Evolution of the voltage of bus 8605 in the 10 476-bus network with a meshed configuration.

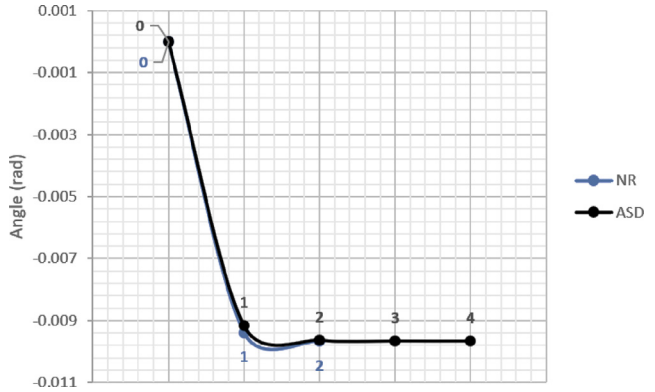

Fig. 18. Evolution of the angle of Bus 8658 in the 10 476-bus network with a meshed configuration.

time required to build the required matrices before the iterative process and the number of iterations required to obtain the solution. However, the ASD algorithm maintains high accuracy and converges, unlike the Gauss–Seidel algorithm. In addition, we can conclude that it can be used in both radial and meshed distribution networks, the latter configuration being the one in which a higher accuracy is obtained. Therefore, it is an algorithm that can be further investigated to be applied in the different electrical grids where distributed renewable energy and electric vehicle charging stations are included, as well as in MV or LV microgrids. Furthermore, this paper can be used as a starting point to investigate the use of the ASD algorithm in unbalanced networks or near the voltage collapse point. Finally, more research is required to select β, which seems to have a great effect on the behavior of the proposed algorithm.

Declaration of competing interest

The authors declare that they have no known competing financial interests or personal relationships that could have appeared to influence the work reported in this paper.

Acknowledgments

The authors would like to acknowledge the support of the CERVERA research program of CDTI, the Industrial and Technological Development Center of Spain, under the research project HySGrid+ (CER-20191019).

References

[1] John J. Grainger, William D. Stevenson, Power System Analysis, McGraw-Hill, 1994.
[2] W. Tinney, C. Hart, Power flow solution by Newton's method, IEEE Trans. Power Appar. Syst. PAS-86 (11) (1967) http://dx.doi.org/10.1109/TPAS.1967.291823.
[3] P.A.N. Garcia, J.L.R. Pereira, S. Carneiro, V.M. Da Costa, Three-phase power flow calculations using the current injection method, IEEE Trans. Power Syst. 15 (2) (2000) http://dx.doi.org/10.1109/59.867133.
[4] N. Costilla-Enriquez, Y. Weng, B. Zhang, Combining Newton–Raphson and stochastic gradient descent for power flow analysis, IEEE Trans. Power Syst. 36 (1) (2021) http://dx.doi.org/10.1109/TPWRS.2020.3029449.
[5] J.C. Hernández, A. Medina, F. Jurado, Optimal allocation and sizing for profitability and voltage enhancement of PV systems on feeders, Renew. Energy 32 (10) (2007) 1768–1789, http://dx.doi.org/10.1016/j.renene.2006.11.003.
[6] F. Lo Franco, M. Ricco, R. Mandrioli, G. Grandi, Electric vehicle aggregate power flow prediction and smart charging system for distributed renewable energy self-consumption optimization, Energies 13 (18) (2020) http://dx.doi.org/10.3390/en13195003.
[7] U.H. Ramadhani, R. Fachrizal, M. Shepero, J. Munkhammar, J. Widén, Probabilistic load flow analysis of electric vehicle smart charging in unbalanced LV distribution systems with residential photovoltaic generation, Sustain. Cities Soc. 72 (May) (2021) http://dx.doi.org/10.1016/j.scs.2021.103043.
[8] V. Boglou, C.S. Karavas, A. Karlis, K. Arvanitis, An intelligent decentralized energy management strategy for the optimal electric vehicles' charging in low-voltage islanded microgrids, Int. J. Energy Res. 46 (3) (2022) 2988–3016, http://dx.doi.org/10.1002/er.7358.
[9] G. Agundis-Tinajero, J. Segundo-Ramírez, N. Visairo-Cruz, M. Savaghebi, J.M. Guerrero, E. Barocio, Power flow modeling of islanded AC microgrids with hierarchical control, Int. J. Electr. Power Energy Syst. 105 (2018) (2019) 28–36, http://dx.doi.org/10.1016/j.ijepes.2018.08.002.
[10] A. Kumar, B.K. Jha, D.K. Dheer, R.K. Misra, D. Singh, A nested-iterative Newton–Raphson based power flow formulation for droop-based islanded microgrids, Electr. Power Syst. Res. 180 (2019) (2020) 106131, http://dx.doi.org/10.1016/j.epsr.2019.106131.
[11] W. Dai, B. Shi, T. Li, H.H. Goh, J. Li, Power flow analysis considering solar road generation, Energy Rep. 8 (2022) 531–536, http://dx.doi.org/10.1016/j.egyr.2022.02.232.
[12] Y. Chen, J. Zhao, J. Ma, Fast decoupled multi-energy flow calculation for integrated energy system, J. Mod. Power Syst. Clean Energy 8 (5) (2020) 951–960, http://dx.doi.org/10.35833/MPCE.2018.000598.
[13] S. Mallick, D.V. Rajan, S.S. Thakur, P. Acharjee, S.P. Ghoshal, Development of a new algorithm for power flow analysis, Int. J. Electr. Power Energy Syst. 33 (8) (2011) 1479–1488, http://dx.doi.org/10.1016/j.ijepes.2011.06.030.
[14] A. Gomez Exposito, A. Conejo, C. Cañizares, Electric Energy Systems: Analysis and Operation, EEUU. Crc Press, ISBN: 0-8493-7365-4, 2008.
[15] S. Ouali, A. Cherkaoui, An improved backward/forward sweep power flow method based on a new network information organization for radial distribution systems, J. Electr. Comput. Eng. 2020 (2020) http://dx.doi.org/10.1155/2020/5643410.
[16] J. Yang, Z. Yun, The thevenin equivalent based power flow method for integrated transmission and radial distribution networks, Int. J. Electr. Power Energy Syst. 123 (June) (2020) 106294, http://dx.doi.org/10.1016/j.ijepes.2020.106294.
[17] A. Garces, A linear three-phase load flow for power distribution systems, IEEE Trans. Power Syst. 31 (1) (2016) 827–828, http://dx.doi.org/10.1109/TPWRS.2015.2394296.

[18] A. Pandey, M. Jereminov, M.R. Wagner, D.M. Bromberg, G. Hug, L. Pileggi, Robust power flow and three-phase power flow analyses, IEEE Trans. Power Syst. 34 (1) (2019) 616–626, http://dx.doi.org/10.1109/TPWRS.2018.2863042.
[19] P. Bannykh, A. Pazderin, Distribution grid three-phase power flow algorithm based on flow model, in: 2020 IEEE 61st Annu. Int. Sci. Conf. Power Electr. Eng. Riga Tech. Univ. RTUCON 2020 - Proc, 2020, http://dx.doi.org/10.1109/RTUCON51174.2020.9316484.
[20] K. Peng, et al., Gauss–Newton hybrid power flow algorithm for AC-DC distribution system, in: China Int. Conf. Electr. Distrib. CICED, 2016-September, No. Ciced, 2016, pp. 10–13, http://dx.doi.org/10.1109/CICED.2016.7576280.
[21] Q. Chen, et al., Power flow analysis of AC-DC networks considering hierarchical connection technique, Int. J. Electr. Power Energy Syst. 115 (2019) (2020) 105493, http://dx.doi.org/10.1016/j.ijepes.2019.105493.
[22] D. Shirmohammadi, H.W. Hong, A. Semlyen, G.X. Luo, A compensation-based power flow method for weakly meshed distribution and transmission networks, IEEE Trans. Power Syst. 3 (2) (1988) http://dx.doi.org/10.1109/59.192932.
[23] G.X. Luo, A. Semlyen, Efficient load flow for large weakly meshed networks, IEEE Trans. Power Syst. 5 (4) (1990) http://dx.doi.org/10.1109/59.99382.
[24] H.D. Chiang, T.Q. Zhao, J.J. Deng, K. Koyanagi, Homotopy-enhanced power flow methods for general distribution networks with distributed generators, IEEE Trans. Power Syst. 29 (1) (2014) http://dx.doi.org/10.1109/TPWRS.2013.2268547.
[25] Y.S. Zhang, H.D. Chiang, Fast newton-FGMRES solver for large-scale power flow study, IEEE Trans. Power Syst. 25 (2) (2010) http://dx.doi.org/10.1109/TPWRS.2009.2036018.
[26] R. Idema, D.J.P. Lahaye, C. Vuik, L. Van Der Sluis, Scalable Newton-Krylov solver for very large power flow problems, IEEE Trans. Power Syst. 27 (1) (2012) http://dx.doi.org/10.1109/TPWRS.2011.2165860.
[27] Y. Chen, C. Shen, A Jacobian-free Newton-GMRES(m) method with adaptive preconditioner and its application for power flow calculations, IEEE Trans. Power Syst. 21 (3) (2006) http://dx.doi.org/10.1109/TPWRS.2006.876696.
[28] F. De León, A. Semlyen, Iterative solvers in the Newton power flow problem: Preconditioners, inexact solutions and partial Jacobian updates, IEE Proc.: Gener. Transm. Distrib. 149 (4) (2002) http://dx.doi.org/10.1049/ip-gtd:20020172.
[29] R.K. Portelinha, C.C. Durce, O.L. Tortelli, E.M. Lourenço, Fast-decoupled power flow method for integrated analysis of transmission and distribution systems, Electr. Power Syst. Res. 196 (2020) (2021) 107215, http://dx.doi.org/10.1016/j.epsr.2021.107215.
[30] K. Li, X. Han, W. Li, R. Ahmed, Unified power flow algorithm of transmission and distribution network, in: 2017 IEEE 6th International Conference on Renewable Energy Research and Applications (ICRERA), 2017, pp. 257–261, http://dx.doi.org/10.1109/ICRERA.2017.8191276.
[31] L. Zhu, S. Chen, W. Mo, Y. Wang, G. Li, G. Chen, Integrated power flow solution for interconnected transmission and distribution network, in: 2019 IEEE 3rd International Electrical and Energy Conference (CIEEC), 2019, pp. 1076–1080, http://dx.doi.org/10.1109/CIEEC47146.2019.CIEEC-2019398.
[32] B. Yang, S. Yang, X. Zhou, X. Cao, Y. Zhi, Y. Ding, A power flow analysis method for the integrated electricity-heat system in distribution network based on forward/backward iterations, in: 2nd IEEE Conf. Energy Internet Energy Syst. Integr. EI2 2018 - Proc, 2018, http://dx.doi.org/10.1109/EI2.2018.8582091.
[33] G.A. Setia, G. Hm Sianipar, K. Samudra, F. Haz, N. Winanti, H.R. Iskandar, Implementation of backward-forward sweep method on load model variation of distribution systems, in: Proc. 2nd Int. Conf. High Volt. Eng. Power Syst. Towar. Sustain. Reliab. Power Deliv. ICHVEPS 2019, 2019, http://dx.doi.org/10.1109/ICHVEPS47643.2019.9011141.
[34] P. Bannykh, S. Lozhkin, N. Mukhlynin, A. Pazderin, O. Malozemova, Distribution grid power flow algorithm based on power-energy flow model, in: 2018 IEEE 59th International Scientific Conference on Power and Electrical Engineering of Riga Technical University (RTUCON), 2018, pp. 1–6, http://dx.doi.org/10.1109/RTUCON.2018.8659860.
[35] D. Borzacchiello, F. Chinesta, M.H. Malik, R. García-Blanco, P. Diez, Unified formulation of a family of iterative solvers for power systems analysis, Electr. Power Syst. Res. 140 (2016) 201–208, http://dx.doi.org/10.1016/j.epsr.2016.06.021.
[36] H.E. Hernandez Fuentes, F.J. Zarco Soto, J.L. Martinez-Ramos, A fast non-decoupled algorithm to solve the load flow problem in meshed distribution networks, in: SEST 2021-4th Int. Conf. Smart Energy Syst. Technol, 2021, http://dx.doi.org/10.1109/SEST50973.2021.9543442.
[37] P. Ladeveze, J. Simmonds, Nonlinear Computational Structural Mechanics: New Approaches and Non-Incremental Methods of Calculation, in: Mechanical Engineering Series, Springer, New York, 1999.
[38] M. Bazrafshan, N. Gatsis, Comprehensive modeling of three-phase distribution systems via the bus admittance matrix, IEEE Trans. Power Syst. 33 (2) (2018) 2015–2029, http://dx.doi.org/10.1109/TPWRS.2017.2728618.
[39] A.G. Expósito, E.R. Ramos, Augmented rectangular load flow model, IEEE Trans. Power Syst. 17 (2) (2002) 271–276, http://dx.doi.org/10.1109/TPWRS.2002.1007892.
[40] K. Rudion, A. Orths, Z.A. Styczynski, K. Strunz, Design of benchmark of medium voltage distribution network for investigation of DG integration, in: 2006 IEEE Power Eng. Soc. Gen. Meet. PES, 2006, p. 6 pp, http://dx.doi.org/10.1109/pes.2006.1709447.
[41] https://pandapower.readthedocs.io/en/v1.2.2/networks/cigre.html.
[42] M.E. Baran, F.F. Wu, Network reconfiguration in distribution systems for loss reduction and load balancing, IEEE Trans. Power Deliv. 4 (2) (1989) 1401–1407, http://dx.doi.org/10.1109/61.25627.
[43] D. Das, Optimal placement of capacitors in radial distribution system using a fuzzy-GA method, Int. J. Electr. Power Energy Syst. 30 (6–7) (2008) http://dx.doi.org/10.1016/j.ijepes.2007.08.004.
[44] H.M. Khodr, F.G. Olsina, P.M.D.O. De Jesus, J.M. Yusta, Maximum savings approach for location and sizing of capacitors in distribution systems, Electr. Power Syst. Res. 78 (7) (2008) 1192–1203, http://dx.doi.org/10.1016/j.epsr.2007.10.002.
[45] The IEEE PES AMPS DSAS Test Feeder Working Group [Online] https://site.ieee.org/pes-testfeeders/resources/.
[46] R.A. Jabr, R. Singh, B.C. Pal, Minimum loss network reconfiguration using mixed-integer convex programming, IEEE Trans. Power Syst. 27 (2) (2012) 1106–1115, http://dx.doi.org/10.1109/TPWRS.2011.2180406.
[47] M.A.N. Guimarães, C.A. Castro, Reconfiguration of distribution systems for loss reduction using Tabu search, in: 15th Power Syst. Comput. Conf. PSCC 2005 (August), 2005, pp. 22–26.
[48] C.T. Su, C.F. Chang, J.P. Chiou, Distribution network reconfiguration for loss reduction by ant colony search algorithm, Electr. Power Syst. Res. 75 (2–3) (2005) 190–199, http://dx.doi.org/10.1016/j.epsr.2005.03.002.